

## Effect of the metal concentration on the structural, mechanical and tribological properties of self-organized a-C:Cu hard nanocomposite coatings

A. Pardo<sup>a\*,d</sup>, J. G. Buijnsters<sup>b</sup>, J. L. Endrino<sup>c</sup>, C. Gómez-Aleixandre<sup>d</sup>, G. Abrasonis<sup>e</sup>,  
R. Bonet<sup>a</sup>, J. Caro<sup>a</sup>

a. Fundació CTM Centre Tecnològic, Manresa. Spain

\* Present address

Tel.: 34-93-8777373

Fax: 34-93-8777374

[ainhoa.pardo@ctm.com.es](mailto:ainhoa.pardo@ctm.com.es)

[jaume.caro@ctm.com.es](mailto:jaume.caro@ctm.com.es)

[raul.bonet@ctm.com.es](mailto:raul.bonet@ctm.com.es)

b. Department of Metallurgy and Materials Engineering

KU Leuven

Kasteelpark Arenberg 44

B-3001 Leuven

Belgium

Tel.: 32-0-16321233

Fax: 34-0-16321991

[Ivan.Buijnsters@mtm.kuleuven.be](mailto:Ivan.Buijnsters@mtm.kuleuven.be)

c. Abengoa Research. Spain

Tel.: 34-95-5637340

Fax:

[jose.endrino@research.abengoa.com](mailto:jose.endrino@research.abengoa.com)

d. Instituto de Ciencia de Materiales de Madrid (ICMM-CSIC). Spain

Tel.: 34-91-3349000

Fax: 34-91-3720623

[cgaleix@icmm.csic.es](mailto:cgaleix@icmm.csic.es)

e. Institute of Ion Beam Physics and Materials Research, Dresden, Germany

Tel.: 49-351260-3578

Fax: 49-3512603285

[g.abrasonis@hzdr.de](mailto:g.abrasonis@hzdr.de)

## **Suggested referees**

1. J. Orwa
2. Carles Corbella
3. R. Nevshupa

## **HIGHLIGHTS**

- Multilayered a-C:Cu films have been synthesized by pulsed filtered cathodic arc deposition
- Effect of Cu content up to 28 at.% on the structure and tribomechanical properties is investigated
- Alternated Cu and C nanolayer self-organization.
- Nanohardness, Young's modulus and plasticity index decrease with Cu content
- Increase in coefficient of friction and film wear with increasing Cu content

## **ABSTRACT**

The influence of the metal content (0-28 at.%) on the structural, mechanical and tribological properties of a-C:Cu films grown by pulsed filtered cathodic arc deposition is investigated. Silicon and AISI 301 stainless steel have been used as substrate materials. The microstructure, composition and bonding structure have been determined by scanning electron microscopy; combined Rutherford backscattered spectroscopy-nuclear reaction analysis; and Raman spectroscopy, respectively. The mechanical and tribological properties have been assessed using nanoindentation and reciprocating sliding (fretting tests) and have them been correlated with the elemental composition of the films. A self-organized multilayered structure consisting of alternating carbon and copper metal nanolayers (thickness in the 25-50 nm range), whose formation is enhanced by the Cu content, is detected. The nanohardness and Young's modulus decrease monotonically with increasing Cu content. A maximum value of the Young's modulus of about 255 GPa is obtained for the metal-free film, whereas it drops to about

174 GPa for the film with a Cu content of 28 at.%. In parallel, a 50% drop in the nanohardness from about 28 GPa towards 14 GPa is observed for these coatings. An increase in the Cu content also produces an increment of the coefficient of friction in reciprocating sliding tests performed against a corundum ball counterbody. As compared to the metal free film, a nearly four times higher coefficient of friction value is detected in the case of a Cu content of 28 at.%. Nevertheless, the carbon-copper composite coatings produced a clear surface protection of the substrate evidenced by a reduced wear loss for Cu contents below 5 at.%.

## **KEYWORDS**

Amorphous carbon, filtered cathodic arc evaporation, multilayered a-C:Cu nanocomposite, mechanical properties, tribological properties

## **INTRODUCTION**

Non-hydrogenated amorphous carbon (a-C) films are distinguished as material for solving multiple tribological problems associated with multi-bladed shaving razors for preventing skin abrasion, engines of racing sport vehicles for achieving maximum endurance, hard disk read heads for preventing against head crushers, and in moulding and cutting tool applications [1]. The drawback of an even broader use of a-C films is the high level of compressive stress (leading to poor adhesion with the substrate) and, in some applications, the lack of functionality of a-C layers due to the relative inertness of carbon. Carbon-based nanocomposite materials can combine toughness, ductility and high hardness together with specific functionalities and thus are recognized as multifunctional wear resistant coatings [2, 3]. The incorporation of alloying elements is

a well known strategy for decreasing the residual stress and therefore increasing the adhesion and wear resistance [4, 5]. The improvement of the properties of a-C films by incorporating carbide-forming and non-carbide forming metals has attracted significant research attention in recent years [6]. The major difference of incorporating carbide forming materials such as silicon, titanium or tungsten, is the modification of the carbon bonding environment. These materials are either incorporated as metal or carbide phases in the carbon matrix. On the other hand, the advantage of incorporating a non-carbide forming metal such as cobalt, silver or copper is the presence of metal nanocrystals in the a-C matrix [7-9], which may account for the high ductility and toughness of these films.

Over the last decade, there has been a specific interest in the formation of copper-carbon nanocomposite films as wear resistant and low friction coatings for tribological applications [10-15]. Furthermore, the incorporation of copper has been reported to reduce the temperature-dependent electrical transport and also to enhance the absorbance of light which could be useful for some photovoltaic applications [13]. The hardness of these films decreases severely with Cu incorporation [16]. Besides, friction is largely dependent on the environmental conditions [17]. Elevated toughness can be achieved by strain release via nanosized metal-based crystallites sliding in the amorphous carbon matrix and the interaction forces at the interfaces between the crystallites and carbon matrix are expected to be very weak [16].

Chemical or physical vapour deposition (CVD or PVD) and hybrid techniques have been used for the synthesis of metal-carbon composite films, including plasma-enhanced CVD [16], ion beam deposition [18], co-sputtering [19], reactive sputtering [20], and pulsed filtered cathodic vacuum arc (PFCVA) [7]. The PFCVA technique is especially suitable for metal incorporation in amorphous carbon layers since it allows a

precise control of the content with no hydrogen or any other reaction gas incorporation. Moreover, the PFCVA technique results in the spontaneous self-organization consisting of alternating C and Cu layers [21], whose periodicity depends on the deposition conditions [22]. The origin of the nano-scaled layering is still not well understood and different models have been proposed in the literature such as segregation due to surface directed spinodal decomposition [23], catalytical action of metal [22], interplay of nucleation, noncarbide forming metal surface segregation, ballistic diffusion and re-sputtering [24], radiation enhanced diffusion [25] or energetic ion sub-plantation [7].

The mechanical relaxing effect observed in metal-carbon multilayered films [12, 26] has motivated this study. Copper has been chosen to be incorporated into carbon matrix because of the almost complete immiscibility of both elements [8].

In order to evaluate the suitability of a-C:Cu nanocomposite thin films in applications where severe damage to the covered substrates is caused, the samples have been tested by reciprocating sliding (fretting tests). Fretting wear takes place when two contacting solid materials undergo a relatively small amplitude oscillating displacement [27]. The main characteristic of the wear produced during reciprocating sliding (fretting tests) is that the size of the contact area of the film exposed to the atmosphere depends on the vibration amplitude, while the contact zone of the spherical counterbody, never contacts with the environment [28]. Although the morphological transitions of the C-Cu multilayer system grown by ionized PVD as function of the metal content have already been studied [7], this study reports for the first time the mechanical and tribological behavior of self-assembled multilayer a-C:Cu thin films grown by pulsed filtered cathodic arc deposition.

## EXPERIMENTAL

a-C and a-C:Cu coatings were grown on Si(100) and AISI 301 stainless steel substrates using a pulsed filtered cathodic arc system (Figure 1, PFCA-450 from Plasma Technology Limited, Hong Kong). In order to reduce the incorporation of detrimental macro-particles in the growing films, this system is provided with two pulsed filtered cathodic arc sources, where the generated arc plasmas are guided into the vacuum chamber by an electromagnetic field applied to the curved ducts. The ducts were biased to +20 V to build up a lateral electrical field while external solenoid coils wrapped around the ducts produced an axial magnetic field of about 200 G. The samples were positioned in the center of the chamber (240 mm away from the exit of the filter duct) and they were negatively biased to different voltages described below. In all the deposition processes the samples were continuously rotated at 1.4 rpm. The base pressure in the vacuum chamber was  $2 \times 10^{-5}$  Torr. The cathodes were ignited using a pulse duration of 3 ms at a frequency of 7.5 Hz.

Before deposition, the samples were cleaned for 10 min by using Cr ion etching while -500 V was applied to the sample. Prior to the deposition of the carbon coatings, a Cr-CrN adhesion film was prepared applying to the substrate a DC bias of -130 V at 80 °C. The two arc sources were ignited on pure chromium rods (99.5%) and an argon flow of 2.5 sccm was introduced into the chamber. A nitrogen flow of 6 sccm was introduced through the arc sources forming a hybrid metal-gas plasma. The pressure during the deposition of CrN was  $8 \times 10^{-4}$  Torr. Total thickness of these layers ranged between 120 and 170 nm (see Table I). The deposition rate was about 1.1 nm/min.

The a-C coatings were prepared at room temperature by using a single cathodic arc source provided with a pure carbon cathode (99.997%). In order to reduce the residual

stress during the initial stage of carbon coating growth, the substrate was biased to a pulsed potential of -1000 V (30 kHz, 10% duty cycle) during the first 40 minutes of the deposition process. In a second stage, a substrate bias of -400 V (30 kHz, 10% duty cycle) was maintained during 140 minutes. Copper-enriched coatings were prepared by the co-evaporation of carbon and copper and using the same two-stage procedure. A pure copper cathode (99.93%) was ignited using the second arc source. The copper concentration in the coatings ranged between 3 at.% and 28 at.% changing the ratio of the main arc current  $I_{\text{Carbon}}/I_{\text{Copper}}$  from 3.4 to 0.8 respectively and keeping the  $I_{\text{Carbon}}$  constant. In all cases, an argon flow of 2.5 sccm was introduced into the chamber and the pressure during the deposition of a:C and a-C:Cu was about  $8 \times 10^{-4}$  Torr. The thickness of the coatings ranged between 510 and 660 nm (see Table I).

The film areal densities of Cu and C were determined by combined Rutherford backscattering spectroscopy (RBS) - nuclear reaction analysis (NRA) measurements using 1.228 MeV deuterium ions. The nuclear reaction  $\text{C}^{12}(\text{d},\text{p})\text{C}^{13}$  cross-section exhibits a maximum at approximately this deuterium ion energy, significantly enhancing the proton signal from carbon, while RBS of deuterium (reaction  $\text{Cu}(\text{d},\text{d})\text{Cu}$ ) from the heavy copper atoms measures the copper content in the deposited layer. The areal densities were estimated using surface approximation from the integrals of Cu and C peaks (for more information on similar measurements see Ref. [29]).

The film morphology has been explored by scanning electron microscopy (SEM). The backscattered electron images of the film cross-sections were taken using a Zeiss Ultra plus microscope.

The bonding structure of the a-C and a-C:Cu coatings was studied by using a Jobin-Yvon Labram HR 800 micro-Raman spectrometer. Unpolarized visible Raman spectra

were recorded in backscattering geometry with a solid state laser emitting at a wavelength of 532 nm in the visible range (VIS). The power at the sample was 1 mW with a 50x objective and the spot diameter at the sample surface was about 1 micron for the visible measurements. Ultra Violet (UV)-Raman spectra were recorded by using a He/Cd laser source at a wavelength of 325 nm. In order to prevent sample damage, the power of the UV source was set below 4 mW with an UV 40x objective. The gratings used for the visible and UV measurements were 600 and 2400 g/mm. The detector used was a CCD cooled at -70 °C.

Nanohardness (H) and Young's modulus (E) of the coatings were measured using a NanoIndenter XP (MTS) system fitted with a Berkovich diamond tip. The tip was calibrated on a fused silica sample using the Oliver and Pharr method [30]. The evaluation of H and E was conducted as function of the depth penetration using the continuous stiffness measurement (CSM) operation mode. During the CSM operation, the AC load was controlled to give a harmonic displacement amplitude of 2 nm at 45 Hz. The samples were allowed to thermally equilibrate with the instrument until the drift rate was below 0.06 nm/s. The indentations were carried out at a constant strain rate of  $0.050 \text{ s}^{-1}$  up to a maximum penetration of 1500 nm in the case of silicon substrates (to prevent substrate cracking) and 5500 nm for the stainless steel substrates. In order to avoid the mechanical influence of the substrate, the intrinsic coating hardness was determined from depth-hardness curves at indentation depth equal or inferior to 10% of the coating thickness. The E values have been taken from the same depth position for which a maximum in H was derived. A Poisson's ratio of 0.25 was assumed for all samples. H and E values were averaged over 20 indents for each sample.



The tribological behaviour of the a-C and a-C:Cu coatings was evaluated by reciprocating sliding (fretting) tests with a relatively small peak-to-peak displacement amplitude (200  $\mu\text{m}$ ). The corundum ball counterbody ( $\alpha\text{-Al}_2\text{O}_3$ , producer: Cerasec (NL),  $\varnothing=10\text{mm}$ ), renewed after each single test, was oscillated at a frequency of 5 Hz at 21 °C and a relative humidity of 50 % using an experimental setup described in detail elsewhere [27]. The experiments were conducted with a normal load of 2 N, 5 N, and 10 N for a total number of 10000 cycles. The linear contact displacement, the normal contact force, and the corresponding friction force were measured as a function of time at preselected sliding cycles [27]. The wear volume loss was evaluated by means of white light interferometry (Wyko NT3300, Veeco, USA).

## RESULTS AND DISCUSSION

The combined RBS-NRA spectra of a-C:Cu films deposited on Si substrates are shown in Fig. 2. One can identify two regions: RBS region (below 200 channels) dominated by backscattering processes and NRA region (above about 200 channels). In the RBS region one can identify the peaks originated from the Cu(d,d)Cu backscattering in the a-C:Cu film, the Cr(d,d)Cr backscattering from the underlying Cr film and the Si(d,d)Si process from the Si substrate. The interaction with C atoms produces a similar signal which is relatively low in intensity due to the low scattering cross-section characteristic for light elements and obscured by a significantly more intense overlapping Si signal. The C signal is separated from that of Si by tuning the incident  $d$  energy to the range where a resonant nuclear reaction is induced. For 1.228 MeV the nuclear reaction  $^{12}\text{C}(\text{d},\text{p})^{13}\text{C} + 2.72 \text{ MeV}$  [31] produces beams of protons which carry part of the reaction energy. The reaction exhibits a large reaction cross-section resulting in an intense peak at high energies (at around channel 530). One can observe that the  $^{12}\text{C}(\text{d},\text{p})^{13}\text{C}$  reaction

peak intensity decreases with increasing Cu content (see Fig. 2) indicating a lower total amount of deposited carbon. The Cu and C areal densities were determined from the area under the peaks corresponding to  $\text{Cu(d,d)Cu}$  and  $^{12}\text{C(d,p)}^{13}\text{C}$  reactions, respectively. The results of the copper content,  $\text{Cu/Cu+C (at.\%)}$ , are gathered in Table I.

Figure 3 shows the cross section SEM images of the copper-free films grown on the silicon substrate (Fig. 3a) and metal containing films with copper contents  $\text{Cu/Cu+C}$  of ~5, 18 and 28 at.% (Figs. 3b to d, respectively). The carbon coating appears as a dense and compact layer above the Cr-based adhesion film. Some droplets are observed on the smooth surface. For a Cu content of 5 at.%, an a-C:Cu nanolayered structure is observed (bright contrast in Fig. 3b). The a-C:Cu with copper to carbon ratio of 18% and 28% shows a similar number of Cu nanolayers (bright contrast, see Figs. 3c and d). The copper is assumed to be in metallic phase [32]. The thickness of the C/Cu periodic structure is in the 25-50 nm range (being thicker the copper layer). In addition, SEM cross section of the films shows that there is a minimum metal content of 5 at.% from which a layered structure can be formed. The a-C:Cu(18) and a-C(28) coatings present the formation of 13 and 12 metal nanolayers, respectively. This periodic structure of alternating metallic Cu and C layers, is not related to the sample rotation during the growth since the periodicity does not match with the substrate holder rotation speed. The rotation speed needed to form a C/Cu nanolayer should be substantially smaller (0.112 rpm) than the actual one (1.4 rpm). Therefore, we attribute the formation of the layered structure to the self-organization process reported in the literature for carbon-transition metal films in general [21-25] and for C:Cu films grown by pulsed filtered cathodic arc in particular [7]. The directionality effects reported in Ref. [7] are averaged out most probably due to the sample rotation. The existence of a minimum metal content to induce such a self-organization process is also consistent with the literature

[29]. Note that the energetic species must be involved in the deposition process [7, 21-25, 29]. This is consistent with the current approach where a flux of hyperthermal is produced at the cathode during arc discharge.

The comparison of the Raman spectra of pure a-C and a-C:Cu(28) samples measured using 325 nm (Fig.4a) and 532 nm (Fig.4b) excitation wave-lengths are shown in Fig. 4. The presented spectra have been intentionally selected to highlight any possible differences in bonding structure arising as due to the metal incorporation into the carbon matrix. The Raman spectra in the 800-1800  $\text{cm}^{-1}$  region shows the so-called G and D peaks. These typical peaks of amorphous carbon films lie at around 1560 and 1360  $\text{cm}^{-1}$  respectively for visible (VIS) excitation, and correspond to in-plane stretching and six-fold ring breathing vibrations of  $\text{sp}^2$  sites [33]. In addition, the T peak at around 1060  $\text{cm}^{-1}$ , associated with C-C  $\text{sp}^3$  vibrations [34, 35], can be hardly observed with UV excitation for a-C:Cu(28) (Fig. 4a). On the other hand, comparing the spectra for both wavelengths, the most remarkable feature is the shift of the D and G peak position upward for the higher excitation energy (325 nm) (Table II). The displacement in the position of the peaks is explained because of the resonance of short strained double bonded carbon chains at higher excitation energies [34].

The penetration depth of the exciting radiation,  $h$ , has been roughly estimated by means of the expression  $h=1/(2\alpha)$ . The absorption coefficient,  $\alpha$ , has been extrapolated from the measurements performed in amorphous carbon films by A. Tamuleviciene *et al* [36]. Penetration depths of 120 nm and 30 nm have been estimated for VIS and UV radiation, respectively. As expected, even in this last case where  $h$  is the same order of the C/Cu period thickness, only the Raman peaks representative of amorphous carbon are detected. This allows the detection of any possible effect of the metal in the carbon structure.

In order to evaluate the position of the G peak as well as the variation of the intensity ratio of the D and G peaks, ( $I_D/I_G$ ) as function of the metal content in the films, the Raman spectra were fitted to two Gaussians. The fitting results of the selected samples are shown in Table II. As can be seen from this table, the G and D peak position remains almost the same regardless of the Cu content. The increase in Cu content does not seem to induce any substantial change in the C phase, which is in agreement with the VIS-Raman observations in the literature [7]. Also note, that due to possible plasmon-polariton enhancement around the copper phase, the significant part of the signal might come from the copper/carbon interfaces. As the interfaces are expected to have similar bonding structure, no considerable changes are observed by increasing carbon content. On the other hand, the slightly higher  $I_D/I_G$  ratio from the a-C:Cu (28) film in comparison to the a-C film (Table II) and the significant, but irregular shift in the D peak position could indicate some ordering and larger degree of six fold ring clustering [6, 33].

The averaged values of the Young's modulus (E) and nanohardness (H) as a function of the relative metal content,  $Cu/(Cu+C)$ , are displayed in Figures 5a and 5b, respectively. The E values have been taken from the same depth positions for which a maximum in hardness was derived. It can be observed that the differences between the values obtained for films deposited either on the silicon (100) or stainless steel substrate are within relative errors, indicating a negligible influence of the substrate material on the nanoindentation measurements. It is evident that there is a monotonous decrease in both H and E with increasing Cu content. A maximum E of about 255 GPa is obtained for the metal-free film, whereas it drops to about 174 GPa for the film with a Cu content of 28 at.%. In parallel, a 50% drop in the H values from about 28 GPa towards 14 GPa is observed for these coatings. The so-called plasticity index, being the ratio of the

nanohardness and Young's modulus (i.e,  $H/E$ ), is frequently used to highlight the elastic-plastic and wear resistance properties of thin films [12, 37]. Here, it is nearly constant in the range 0.10-0.11 for the a-C film and a-C:Cu composite films with a Cu content up to 5 at.%, whereas lower  $H/E$  values of 0.095 and 0.084 are derived for samples a-C:Cu(18) and a-C:Cu(28), respectively (Fig. 5c). Musil et al. [38] reported a similar decrease in the resistance of plastic deformation ( $H^3/E^2$ ) with increasing Cu content of sputtered a-C/Cu films. Overall, the measured values for  $H$ ,  $E$  and  $H/E$  are very similar to those reported in a previous study by Dwivedi *et al.* [12]. They found  $H$  and  $E$  values in the range 18-27 GPa and 220-280 GPa, respectively, and a maximum  $H/E$  value of about 0.093 for Cu/DLC bi-layer films deposited by using a hybrid system involving plasma enhanced CVD and RF-sputtering. In several other studies [16, 39] C:Cu nanocomposite films with a relatively soft polymer-like hydrogenated carbon matrix were investigated. This facts disable a direct comparison with our films.

The loops obtained during the reciprocating sliding (fretting tests) are shown in Fig. 6. They represent the tangential force versus the displacement of a-C and a-C:Cu films deposited onto stainless steel substrates. All the logs present a constant force as soon as a full sliding is achieved. This produces the characteristic rectangular shape of the gross-slip regime [28]. The log of the substrate is considerably larger than those of the coated substrates, which clearly indicates a reduction in sliding friction when the substrate is coated. In addition, this difference in size suggests a markedly protection role exerted on the substrate by both the a-C and the a-C:Cu films. Conversely, the area of the logs, related to the dissipated energy during the sliding cycle and with the coefficient of friction (CoF) of the samples [40], tends to increase with the Cu content.

The CoF has been determined from the value of the friction force (dissipated energy,  $E_d$ , in a loop) corresponding to a preselected number of cycles ( $\text{CoF} =$

$E_d/(2 \cdot \text{displacement} \cdot F_N)$ ) [40]. Fig. 7 shows the CoF for a-C and a-C:Cu samples applying 2N normal load (Fig. 7a), and only for a-C:Cu(3) applying normal loads of 2N, 5N and 10N (Fig. 7b). The CoF during the first cycles of the tests vary from 0.05 for the a-C film, up to 0.10 for a-C:Cu(28) which indicates an increment of the initial friction force with the metal content in the first stages of the tests (Fig. 7a). The metal free a-C layer remains with a value under 0.1 during the complete 10000 cycle test. In the other stages, the progressive increase of CoF concomitantly with the sliding cycles can be associated with the increase of the actual contact area between the two counterfaces related to the gradual penetration of the counterbody into the film [16, 41]. An increment in the CoF with the Cu content is observed (see Fig. 7a). This may be explained by considering the mechanical properties of the coatings: as the Cu content increases, the decrease in the resistance to plastic deformation may induce an easier penetration of the counterbody into the a-C:Cu films leading to the increment in the CoF.

The effect of the variation of the normal load on the CoF is shown in Fig. 7b for the case of the a-C:Cu(3) film. As the normal load increases the CoF decreases. As proposed in the literature for metal free [40] and metal containing hydrogenated amorphous carbon [42], this effect may be related to a lower interaction with the environment by increasing load.

The wear tracks, the penetration depth and the volume loss after the fretting tests have been studied by white light interferometry. As can be seen in Fig. 8, all the tracks present the characteristic ellipse-shape of fretting tests [42]. However, a noticeable difference in the size of the wear tracks formed after a 10000 cycles at 2N normal load tests is detected for Cu contents above 5 at.%. The largest wear track is formed on the pristine substrate (Fig. 8a). The depth profiles presented in Fig. 8e, confirm that all the

coatings show a protective effect. Even the a-C:Cu(28) sample shows a wear track size comparable to that of the substrate one, the depth profile is significantly shallower. Note that the maximum values of the wear depth are significantly smaller than those of the film thickness for the a-C and a-C:Cu(3) films, while it is similar for the a-C:Cu(28) film (see Table I). The latter can also explain the somewhat unexpected behavior in the CoF starting from about 6.000 cycles.

The variation of the volume loss,  $V_{\text{loss}}$ , as function of the Cu content and the accumulated dissipated energy,  $E_d$ , after the fretting tests for 2N, 5N and 10N normal loads have been derived from white light interferometry measurements and the fretting loops respectively (see Fig. 9). As expected, for a certain Cu content, both  $V_{\text{loss}}$  and  $E_d$  increase due to the stronger penetration of the counterbody into the film. For the three tested normal loads, both magnitudes also increase with the metal content, which is in agreement with the decrease of the resistance to the plastic deformation and the increase of the CoF with the Cu content, reported above.

The top-view SEM images of the wear tracks in a-C and a-C:Cu films, after 10000 cycles applying 2N normal load, are shown in Fig. 10. Usually, the carbon films grown by PVD reproduce the stainless steel surface topography. The high roughness of the substrate becomes more evident in the central part of the wear tracks caused by the thinning of the film as a result of the wear caused by the repeated sliding of the counterbody. There is no evidence of scratches, wear particles or worn material in the vicinity of the wear track in a-C and in a-C:Cu(5) (Figs. 10 a.1, a.2, b.1 and b.2). On the contrary, the scratches become visible along the sliding direction and the worn material is accumulated on the sides of the wear track when the Cu content is higher, i.e. for a-C:Cu(18) and a-C:Cu(28) films (Figs. 10c.1 and d.1, respectively). It can be seen in Fig. 10c.2 and 10d.2 how the worn material is plastically deformed, swept along with the

counterbody and finally piled up. This effect is accentuated at the beginning (or at the end) of the reciprocating sliding displacement (200  $\mu\text{m}$ ). Even for the a-C:Cu(28) film, the worn material is accumulated on the sides of the wear track perpendicular to the movement. The amassment of material seems to be enhanced when the Cu content is higher in the films since the accumulation is clearly superior in the sample with the highest Cu content (Fig.10 d.2). This is consistent with the observations above that the increase of Cu content in the films diminishes the resistance to plastic deformation (Fig. 5c). During a reciprocating sliding test, the higher the Cu content, the easier is the penetration of the counterbody into the coating. This favours the wear of the film, increasing the wear track size and therefore the material loss during the experiment.

## CONCLUSIONS

a-C:Cu thin films with different Cu content (0-28 at. %) were obtained by PFCA using a two-stage procedure. Above a certain critical metal content (5 at.%) a self-organized layered film morphology forms. The coated samples present superior mechanical properties compared to the bare Si and stainless steel substrates. However, increasing the Cu at.% produces: a decrease in Young's modulus from 255 GPa for a-C, to 174 GPa for a-C:Cu(28); a 50% drop in nanohardness (from 28 GPa to 14 GPa respectively); an increment of coefficient of friction nearly four times in reciprocating sliding tests in the 0-28 at.% range. Increasing the Cu content produces a decrease in the resistance to plastic deformation. This induces an easier penetration of the counterbody into the a-C:Cu films leading to the increment of friction and wear. In conclusion, adding amounts of copper above ~5% at. in a-C films results in a worsening of the tribological properties in terms of hardness, friction and fretting wear- resistance.



However, for many industrial applications the adhesion, the residual stress and the fracture toughness of the coating play an important role in the performance of the coatings. As stated previously, it is expected that the incorporation of a non-carbide forming metal such as copper can improve these properties. Consequently, future work will be addressed to study the influence of the copper addition in the fracture toughness, the stress release and adhesion of a-C films grown by PFCA deposition technique.

## **ACKNOWLEDGEMENTS**

This work has been partially financed by the CONSOLIDER Spanish National Project (FUNCOAT, ref: CSD2008-00023). The authors express their gratitude to Professor Jean Pierre Célis from KU Leuven for tribological discussions and also to Dr. Tariq Jawhari from Scientific and Technological Services (University of Barcelona) for the Raman measurements. J.G.B. would like to thank the Executive Research Agency of the European Union for funding under the Marie Curie IEF grant number 272448.

## **REFERENCES**

- [1] A. Erdemir, C. Donnet, Tribology of diamond-like carbon films: recent progress and future prospects, *Journal of Physics D: Applied Physics*, 39 (2006) 311-327.
- [2] S.V. Hainsworth, N.J. Uhure, Diamond like carbon coatings for tribology: production techniques, characterisation methods and applications, *International Materials Reviews*, 52 (2007) 153-174.
- [3] C.A. Charitidis, Nanomechanical and nanotribological properties of carbon-based thin films: A review, *International Journal of Refractory Metals and Hard Materials*, 28 (2010) 51-70.

- [4] J. Musil, P. Novak, R. Cerstvy, Z. Soukup, Tribological and mechanical properties of nanocrystalline-TiC/a-C nanocomposite thin films, *Journal of Vacuum Science & Technology A*, 28 (2010) 244-249.
- [5] S. Zhou, L. Wang, Q. Xue, Duplex doped nanocomposite carbon-based coating with self-lubricating performance, *Diamond and Related Materials*, 21 (2012) 58-65.
- [6] M. Berndt, G. Abrasonis, G.J. Kovács, M. Krause, F. Munnik, R. Heller, A. Kolitsch, W. Möller, Bulk diffusion induced structural modifications of carbon-transition metal nanocomposite films, *Journal of Applied Physics*, 109 (2011) 063503.
- [7] G. Abrasonis, G.J. Kovács, M.D. Tucker, R. Heller, M. Krause, M.C. Guenette, F. Munnik, J. Lehmann, A. Tadich, B.C.C. Cowie, L. Thomsen, M.M.M. Bilek, W. Möller, Sculpting nanoscale precipitation patterns in nanocomposite thin films via hyperthermal ion deposition, *Applied Physics Letters*, 97 (2010) 163108.
- [8] M. Berndt, M. Krause, G. Abrasonis, A. Mücklich, F. Munnik, A. Kolitsch, W. Möller, Morphology and Structure of C:Co, C:V, and C:Cu Nanocomposite Films, *Plasma Processes and Polymers*, 6 (2009) 902-906.
- [9] H. Zutz, I. Gerhards, C. Ronning, H. Hofsäss, M. Seibt, W.-Y. Wu, J.-M. Ting, Self-Organized Nanoscale Multilayer Growth during the Deposition of Hyperthermal Species, *Reviews on Advanced Materials Science*, 15 (2007) 241-246.
- [10] N. Dwivedi, S. Kumar, H.K. Malik, C.M.S. Rauthan, O.S. Panwar, Role of Sandwich Cu Layer in and Effect of Self-Bias on Nanomechanical Properties of Copper/Diamond-Like Carbon Bilayer Films, *ISRN Nanotechnology*, 2011 (2011) 1-7.
- [11] N. Dwivedi, S. Kumar, Ishpal, S. Dayal, Govind, C.M.S. Rauthan, O.S. Panwar, Studies of nanostructured copper/hydrogenated amorphous carbon multilayer films, *Journal of Alloys and Compounds*, 509 (2011) 1285-1293.
- [12] N. Dwivedi, S. Kumar, Nanoindentation testing on copper/diamond-like carbon bilayer films, *Current Applied Physics*, 12 (2012) 247-253.
- [13] N. Dwivedi, S. Kumar, H.K. Malik, C. Sreekumar, S. Dayal, C.M.S. Rauthan, O.S. Panwar, Investigation of properties of Cu containing DLC films produced by PECVD process, *Journal of Physics and Chemistry of Solids*, 73 (2012) 308-316.
- [14] Y. Pauleau, F. Thiéry, V.V. Uglov, V.M. Anishchik, A.K. Kuleshov, M.P. Samtsov, Tribological properties of copper/carbon films formed by microwave plasma-assisted deposition techniques, *Surface and Coatings Technology*, 180-181 (2004) 102-107.

- [15] C.-C. Chen, F.C.-N. Hong, Structure and properties of diamond-like carbon nanocomposite films containing copper nanoparticles, *Applied Surface Science*, 242 (2005) 261-269.
- [16] Y. Pauleau, F. Thiéry, P.B. Barna, F. Misjak, A. Kovacs, S.N. Dub, V.V. Uglov, A.K. Kuleshov, Nanostructured copper/hydrogenated amorphous carbon composite film prepared by microwave plasma-assisted deposition process from acetylene-argon gas mixtures, *Reviews on Advanced Materials Science*, 6 (2004) 140-149.
- [17] R.M. Balestra, A.M.G. Castro, M. Evaristo, A. Escudeiro, P. Mutafov, T. Polcar, A. Cavaleiro, Carbon-based coatings doped by copper: Tribological and mechanical behavior in olive oil lubrication, *Surface and Coatings Technology*, 205 (2011) S79-S83.
- [18] H. Zutz, D. Lyzwa, C. Ronning, M. Seibt, H. Hofsass, Self-organized formation of layered carbon-copper nanocomposite films by ion deposition, *Nuclear Instruments and Methods in Physics Research Section B: Beam Interactions with Materials and Atoms*, 267 (2009) 1356-1359.
- [19] S. Zhang, X.L. Bui, J. Jiang, X. Li, Microstructure and tribological properties of magnetron sputtered nc-TiC/a-C nanocomposite, *Surface and Coatings Technology*, 198 (2005) 206-211.
- [20] M. Samuelsson, K. Sarakinos, H. Högborg, E. Lewin, U. Jansson, B. Wälivaara, H. Ljungcrantz, U. Helmersson, Growth of Ti-C nanocomposite films by reactive high power impulse magnetron sputtering under industrial conditions, *Surface and Coatings Technology*, 206 (2012) 2396-2402.
- [21] J.Y. Jao, S. Han, L.S. Chang, Y.-C. Chen, C.-L. Chang, H.C. Shih, Formation and characterization of DLC:Cr:Cu multi-layers coating using cathodic arc evaporation, *Diamond and Related Materials*, 18 (2009) 368-373.
- [22] W.-Y. Wu, J.-M. Ting, Self-assembled alternating nano-scaled layers of carbon and metal, *Chemical Physics Letters*, 388 (2004) 312-315.
- [23] C. Corbella, B. Echebarria, L. Ramírez-Piscina, E. Pascual, J.L. Andújar, E. Bertran, Spontaneous formation of nanometric multilayers of metal-carbon films by up-hill diffusion during growth, *Applied Physics Letters*, 87 (2005) 213117.
- [24] I. Gerhards, H. Stillrich, C. Ronning, H. Hofsäss, M. Seibt, Self-organized nanoscale multilayer growth in hyperthermal ion deposition, *Physical Review B* 70 (2004) 245418.

- [25] C.Q. Chen, Y.T. Pei, K.P. Shaha, J.Th.M. De Hosson, Tunable self-organization of nanocomposite multilayers, *Applied Physics Letters*, 96 (2010) 073103.
- [26] E. Bertran, C. Corbella, A. Pinyol, M. Vives, J.L. Andújar, Comparative study of metal/amorphous-carbon multilayer structures produced by magnetron sputtering, *Diamond and Related Materials*, 12 (2003) 1008-1012.
- [27] H. Mohrbacher, J.P. Celis, J.R. Roos, Laboratory testing of displacement and load induced fretting, *Tribology International*, 28 (1995) 269-278.
- [28] B. Blanpain, H. Mohrbacher, E. Liu, J.P. Celis, J.R. Roos, Hard coatings under vibrational contact conditions, *Surface and Coatings Technology*, 74-75 (1995) 953-958.
- [29] G. Abrasonis, T.W.H. Oates, G.J. Kovács, J. Grenzer, P.O.A. Persson, K.-H.H. Heinig, A. Martinavicius, N. Jeutter, C. Baecht, M. Tucker, M.M.M. Bilek, W. Möller, Nanoscale precipitation patterns in carbon-nickel nanocomposite thin films: Period and tilt control via ion energy and deposition angle, *Journal of Applied Physics*, 108 (2010) 043503.
- [30] W.C. Oliver, G.M. Pharr, An improved technique for determining hardness and elastic modulus using load and displacement sensing indentation experiments, *Journal of Materials Research*, 7 (1992) 1564-1583.
- [31] J.R. Tesmer, M. A. Nastasi, *Handbook of Modern Ion Beam Materials Analysis*, Materials Research Society 1995, Pittsburg Pennsylvania, 1995.
- [32] J.L. Endrino, D. Horwat, R. Gago, J. Andersson, Y.S. Liu, J. Guo, A. Anders, Electronic structure and conductivity of nanocomposite metal (Au, Ag, Cu, Mo)-containing amorphous carbon films, *Solid State Sciences*, 11 (2009) 1742-1746.
- [33] A.C. Ferrari, J. Robertson, Interpretation of Raman spectra of disordered and amorphous carbon, *Physical Review B*, 61 (2000) 14095-14107.
- [34] A.C. Ferrari, J. Robertson, Resonant Raman spectroscopy of disordered, amorphous, and diamondlike carbon, *Physical Review B* 64 (2001) 075414.
- [35] A.C. Ferrari, B. Kleinsorge, G. Adamopoulos, J. Robertson, W.I. Milne, V. Stolojan, L.M. Brown, A. LiBassi, B.K. Tanner, Determination of bonding in amorphous carbon by electron energy loss spectroscopy, Raman scattering and X-ray reflectivity, *Journal of Non-Crystalline Solids*, 266-269 (2000) 765-768.
- [36] A. Tamuleviciene, S. Meskinis, V. Kopustinskas, S. Tamulevicius, Diamond like Carbon Film as Potential Antireflective Coating for Silicon Solar Cell, *Materials Science (Medziagotyra)*, 16 (2010) 103-107.

- [37] P. Gupta, E.I. Meletis, Tribological behavior of plasma-enhanced CVD a-C:H films. Part II: multilayers, *Tribology International*, 37 (2004) 1031-1038.
- [38] J. Musil, M. Louda, Z. Soukup, M. Kubásek, Relationship between mechanical properties and coefficient of friction of sputtered a-C/Cu composite thin films, *Diamond and Related Materials*, 17 (2008) 1905-1911.
- [39] V.V. Uglov, A.K. Kuleshov, M.V. Astashynskaya, V.M. Anishchik, S.N. Dub, F. Thiery, Y. Pauleau, Mechanical properties of copper/carbon nanocomposite films formed by microwave plasma assisted deposition techniques from argon-methane and argon-acetylene gas mixtures, *Composites Science and Technology*, 65 (2005) 785-791.
- [40] T. Van der Donck, M. Muchlado, W. Zein Eddine, S. Achanta, N.J.M. Carvalho, J.P. Celis, Effect of hydrogen content in a-C:H coatings on their tribological behaviour at room temperature up to 150 °C, *Surface and Coatings Technology*, 203 (2009) 3472-3479.
- [41] V. Singh, J.C. Jiang, E.I. Meletis, Cr-diamondlike carbon nanocomposite films: Synthesis, characterization and properties, *Thin Solid Films*, 489 (2005) 150-158.
- [42] A. Pardo, C. Gómez-Aleixandre, J.P. Celis, J.G. Buijnsters, Friction and wear behaviour of plasma assisted chemical vapour deposited nanocomposites made of metal nanoparticles embedded in a hydrogenated amorphous carbon matrix, *Surface and Coatings Technology*, 206 (2012) 3116-3124.

## Figures

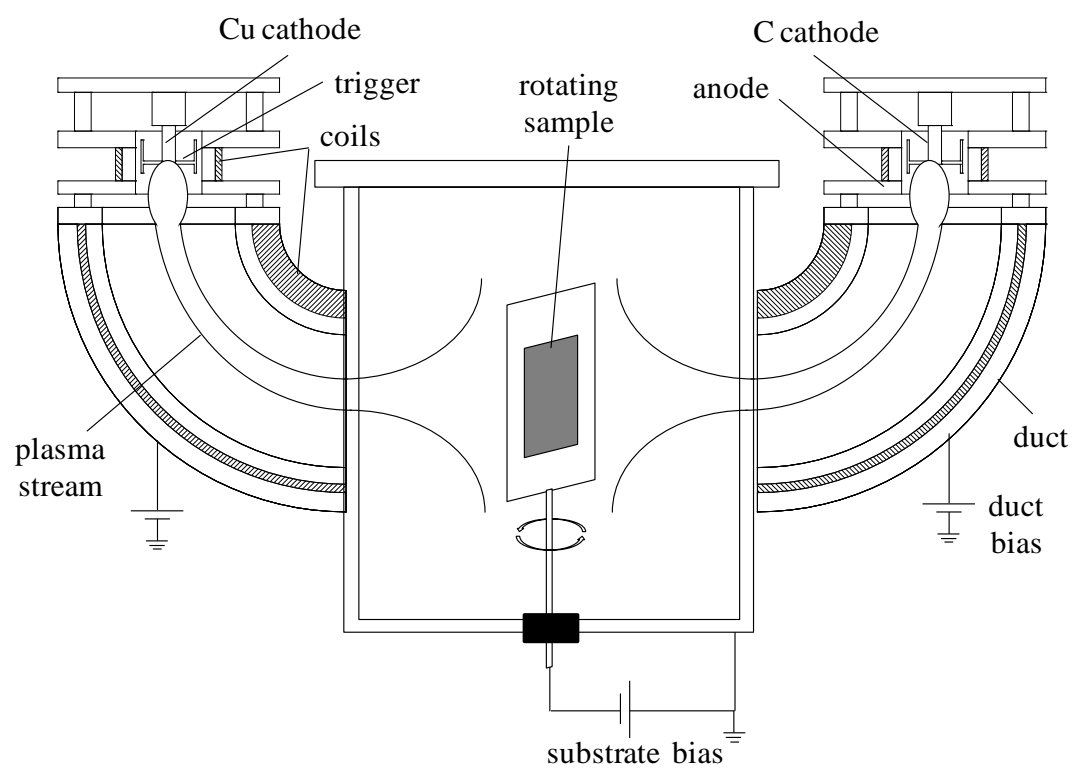


**Fig.1.** Schematic of the pulsed filtered cathodic arc system.

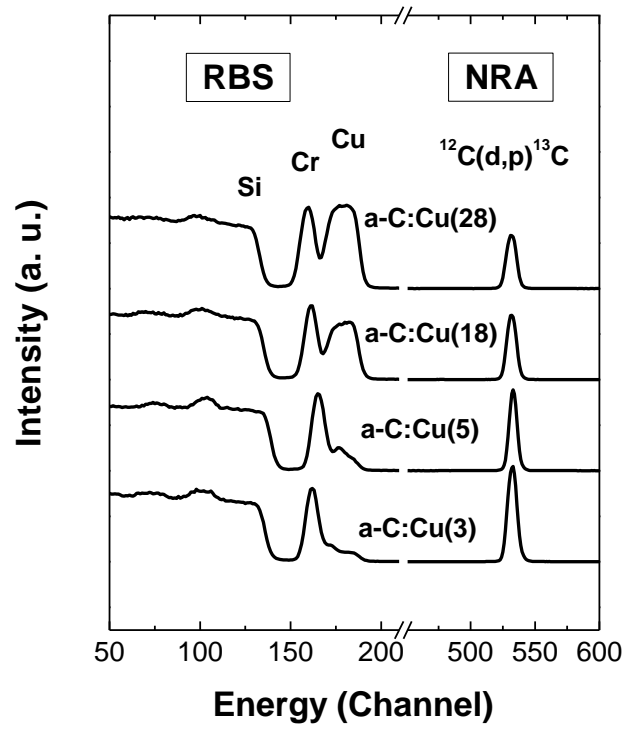


**Fig.2.** Combined RBS-NRA spectra obtained from a-C:Cu samples deposited on Si substrates.

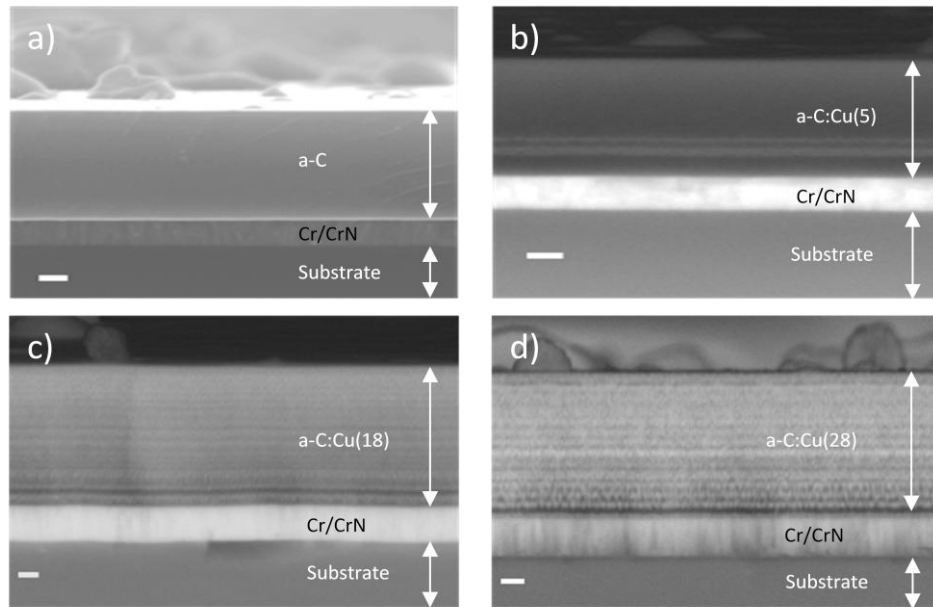


**Fig.3.** Cross section SEM images of samples: a) a-C, b) a-C:Cu(5), c) a-C:Cu(18) and d) a-C:Cu(28). Scale bar of 100 nm.

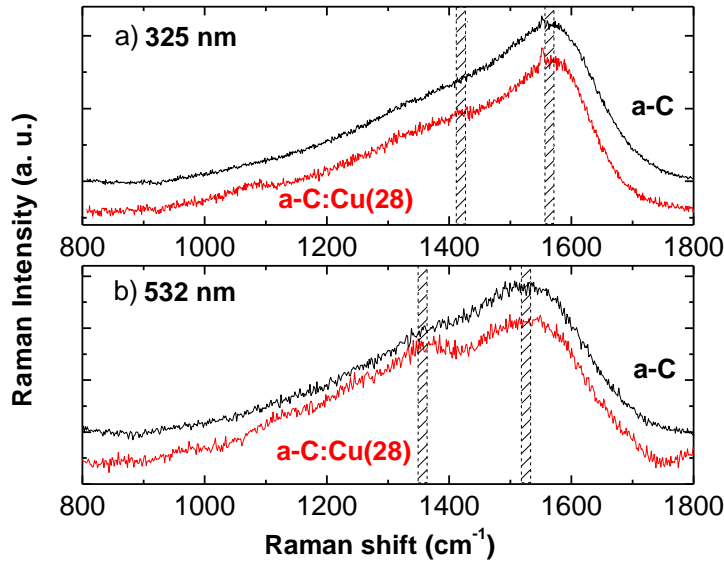


**Fig.4.** a) UV (325 nm) and b) Visible (532 nm) Raman spectra obtained from the a-C and the a-C:Cu(28) samples. The positions of the D and G peaks are indicated by the vertical dashed zones.

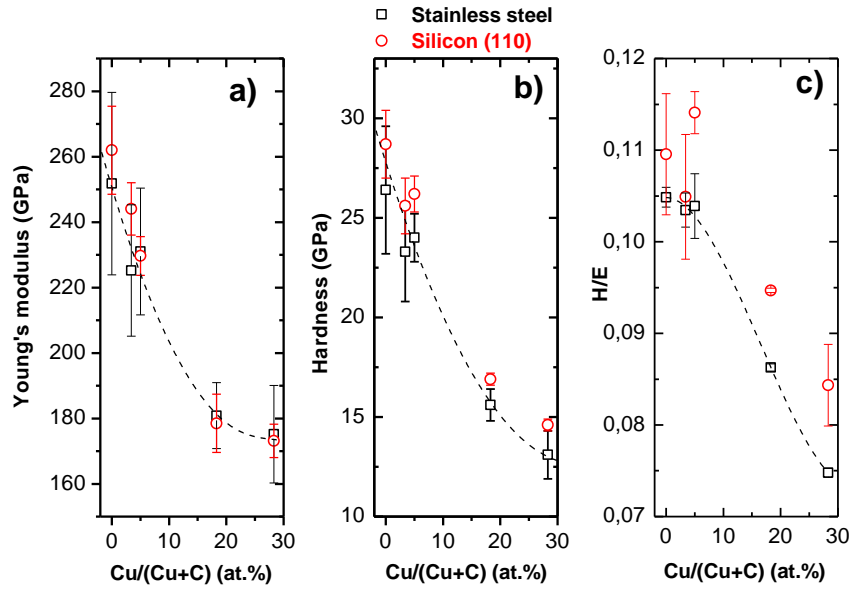


**Fig.5.** a) Young's modulus (E), b) hardness (H), and c) H/E ratio derived from nanoindentation measurements on a-C:Cu samples on stainless steel (squares) and on silicon (circles) as function of Cu content.



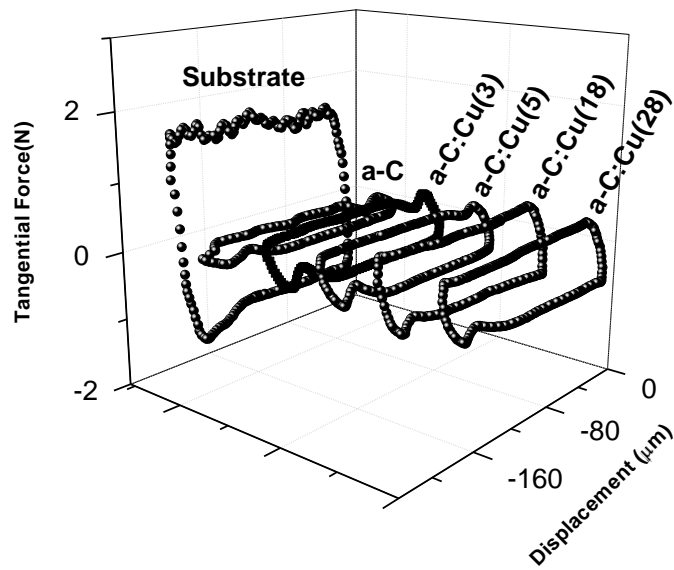


**Fig.6.** Fretting logs (tangential force vs displacement) measured after 10.000 sliding cycles applying 2N normal load on a-C and a-C:Cu samples covering a stainless steel substrate.

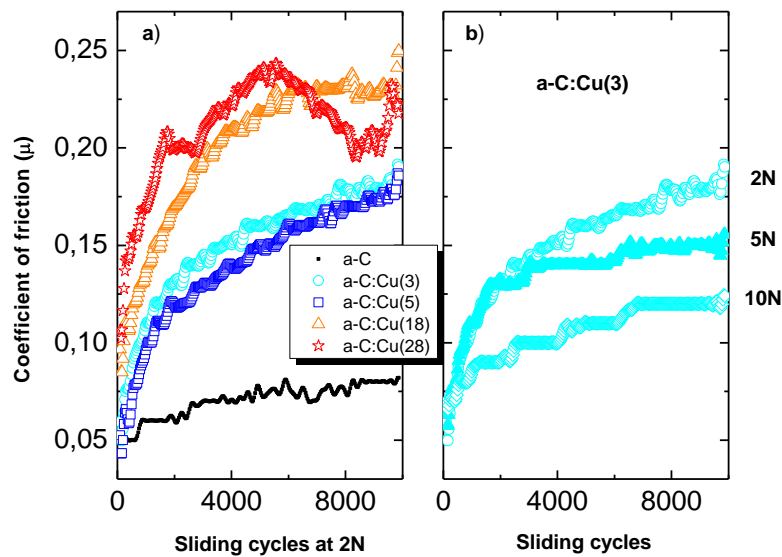


**Fig.7.** Coefficient of friction as function of sliding cycles: a) applying 2N normal load on a-C and a-C:Cu samples, and b) applying 2, 5 and 10 N on a-C:Cu(3). Stainless steel was used as substrate material in all cases.

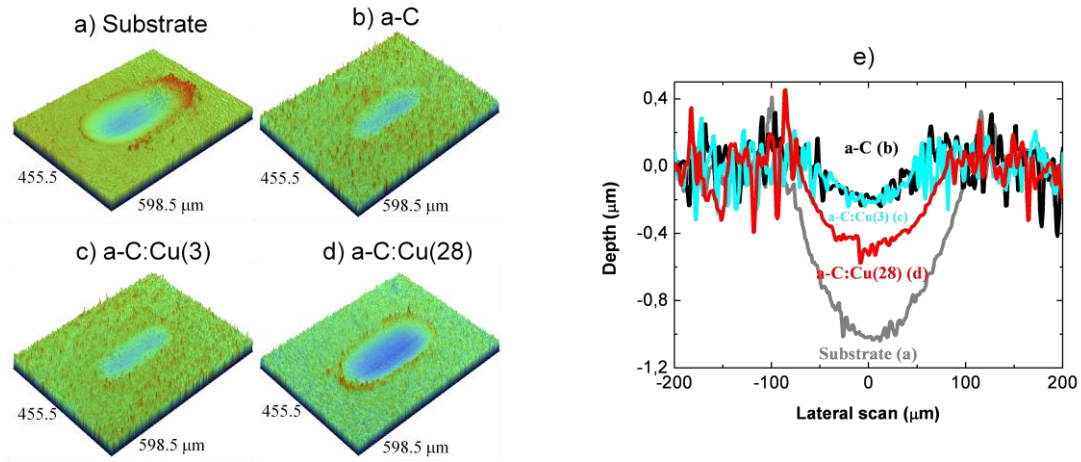


**Fig.8.** White light interferometry images of the wear tracks formed after the fretting tests performed applying 2N normal load during 10.000 cycles on: a) the stainless steel substrate, and b) a-C, c) a-C:Cu(3), and d) a-C:Cu(28) samples. e) Depth profiles of the different wear tracks.

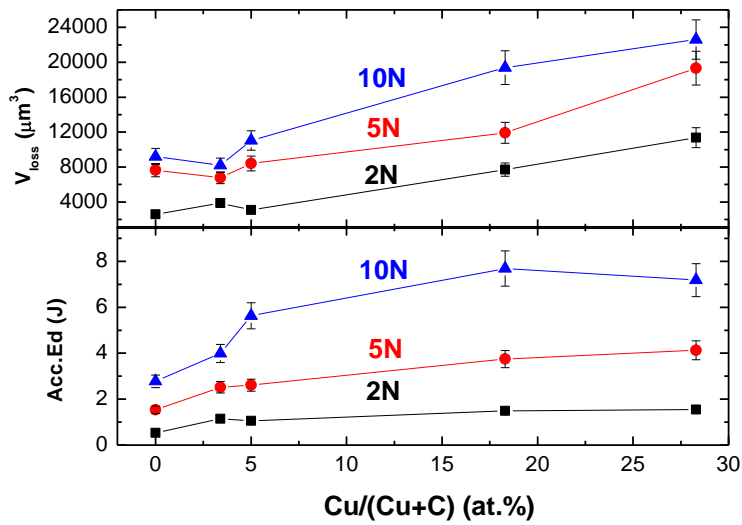


**Fig.9.** Volume loss ( $V_{\text{loss}}$ ) and accumulated dissipated energy (Acc.Ed) as function of the Cu content obtained after 10000 fretting cycles applying 2, 5 and 10 N normal loads.

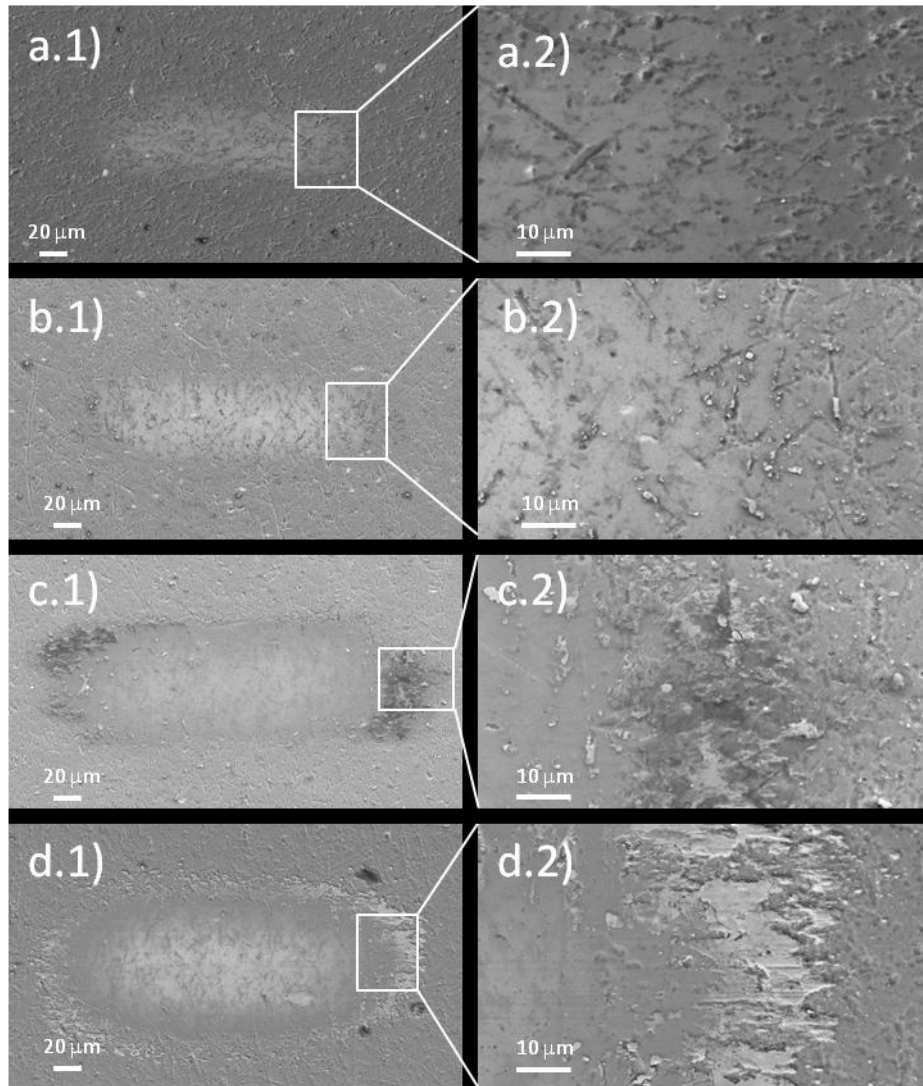


**Fig.10.** SEM images of the wear tracks formed after 10000 cycles of reciprocating sliding applying 2N normal load on the: a) a-C, b) a-C:Cu(5), c) a-C:Cu(18) and d) a-C:Cu(28) coatings.

## Tables

**Table I.** Cu content (in at.%) measured by NRA, thickness of the a-C and a-C:Cu films, the Cr-CrN interlayer and total film thickness for the studied samples.

Sample	Cu/(Cu+C) (at.%)	a-C:Cu film thickness (nm)	Cr-CrN interlayer thickness (nm)	Total thickness (nm)
a-C	0	610	140	750
a-C:Cu(3)	3	660	120	780
a-C:Cu(5)	5	510	145	655
a-C:Cu(18)	18	660	170	830
a-C:Cu(28)	28	610	160	770

**Table II.** Position of D, G and T Raman peaks and  $I_D/I_G$  obtained by a fitting of the spectra to two (532 nm) or three (325 nm) Gaussian functions for the a-C and a-C:Cu(28) samples.

Sample	D position ( $\text{cm}^{-1}$ )		G position ( $\text{cm}^{-1}$ )		T position ( $\text{cm}^{-1}$ )	$I_D/I_G$	
	325 nm	532 nm	325 nm	532 nm	325 nm	325 nm	532 nm
a-C	$1419 \pm 4$	$1395 \pm 9$	$1575 \pm 4$	$1556 \pm 7$	-	1.00	1.23
a-C:Cu(28)	$1437 \pm 3$	$1373 \pm 8$	$1578 \pm 4$	$1560 \pm 10$	$1070 \pm 10$	1.04	1.38